Analysis of Metal-Plate-Connected Wood Trusses with Semi-rigid Joints

R. Gupta, K. G. Gebremedhin, J. R. Cooke
Member ASAE, Member ASAE, Fellow ASAE

Abstract

Metal-plate-connected wood trusses with semi-rigid joints were investigated by the matrix method of structural analysis. The element-stiffness matrix and fixed-end forces of an individual member with one or both ends semi-rigid were derived as modifications of the idealized cases. The case of unequal elastic connections at two ends of a member can also be handled by this method of analysis. When one end is semi-rigid, the other end may be specified as pinned, rigid, or semi-rigid. The truss was analyzed for three different joint assumptions: pin, rigid, and semi-rigid joints. The truss performance, based on deflection, varied greatly depending on the joint assumption. Including semi-rigid-joint behavior in the analysis of a wood truss decreased maximum deflection by 34% compared with the pinned-joint assumption and maximum moment by 13% compared with the rigid-joint assumption. By incorporating semi-rigid behavior of joints, more accurate member forces can be obtained enabling closer prediction of actual truss behavior. **Keywords.** Wood engineering, Matrix method, Element-stiffness matrix, Fixed-end forces.

Introduction

Conventional procedures for the analysis of wood trusses are based on the assumption that the member-end connections are either pinned or completely rigid. Although these assumptions are not entirely consistent with actual conditions, they have been accepted because they simplify analysis and design. The actual connections of wood trusses are semi-rigid, allowing some relative movement between the joined members in the plane of the truss. The movement may be axial, translational, or rotational due to concentric or eccentric forces in the members. Axial or rotational deformation of the joints can be responsible for a substantial proportion of the overall deformation of a structure and often has a significant bearing on the internal force distribution.

The majority of light-frame trusses are designed and manufactured in accordance with the recommendations of the Truss Plate Institute (1985). In the simplified method (empirical analysis), generally considered to be conservative, Truss Plate Institute (1985) recommends the use of buckling and moment-length factor for designing top and bottom members. This method has been developed based upon many years of experience in wood truss design and extensive investigation using the Purdue Plane Structures Analyzer (PPSA) on standard truss configurations. Several researchers (Maraghechi and Itani, 1984; Lau, 1987; Masse and Salinas, 1988) have simulated the behavior of semi-rigid connections by means of equivalent "springs" or "fictitious members". This method either estimates or calibrates the dimensions of the fictitious members according to joint stiffness. Another way to include the behavior of semi-rigid connections in the analysis is to modify the stiffness properties of the individual members having a semi-rigid connection at one or both ends (Weaver and Gere, 1986; Fu and Seckin, 1988; Sasaki et al., 1988). This means modifying the fixed-end forces and stiffness matrices of the members. The most notable work on modeling the mechanics of metal-plate-connected truss joint performance was developed by Foschi (1977) and modified by Triche and Suddarth (1988). Cramer and Wolfe (1989) have developed a load-distribution model for light-frame wood roof assemblies with metal-plate-connected trusses, in which truss connections were simulated with simple hinged connections.

Structural characteristics of joints are derived from full scale tests. Maraghechi and Itani (1984) reported that axial and rotational stiffnesses of joints have appreciable influence on member forces, while shear stiffness has little effect. Lau (1987) determined the strength and stiffness values for heel joints from laboratory tests and used these values in a computer program for analysis of wood frames. Gupta (1990) tested tension splice joints, heel joints, and web joints to determine their strength and stiffness.

An alternative method of analysis of wood trusses, connected by metal plates, is presented. The specific objectives of this article are to:

- Include the semi-rigid behavior of joints in the matrix method of analysis of trusses by modifying the fixed-end forces (FEF) and element-stiffness matrix (ESM) to include the axial and rotational stiffnesses of the connections.
- Compare the truss performance predicted by using the semi-rigid joint analysis to truss performance predicted by traditional pinned and rigid connections.

Article was submitted for publication in August 1991; reviewed and approved for publication by the Structures and Environment Div. of ASAE in March 1992. Presented as ASAE Paper No. 90-4527.

Paper 2774 of the Forest Research Laboratory, Oregon State University, Corvallis.

The authors are **Rakesh Gupta**, Assistant Professor, Dept. of Forest Products, Oregon State University, Corvallis; **Kifle G. Gebremedhin**, Associate Professor, and **J. Robert Cooke**, Professor, Agricultural and Biological Engineering Dept., Cornell University, Ithaca, NY.

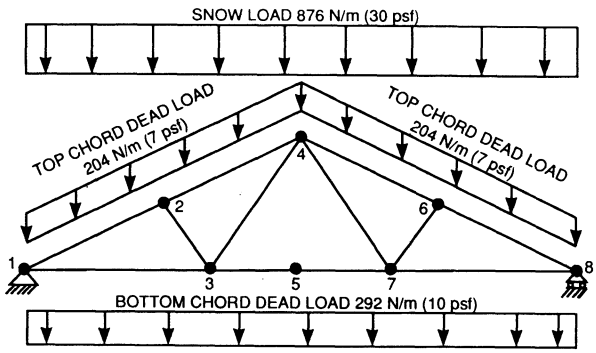

Figure 1–Fink truss analog with design loads. Joints 1 and 8 are heel joints; 3 and 7 are web joints; and 5 is a tension splice joint.

Modified FEF and ESM are derived as modifications of the idealized cases. Similar derivations have previously been done by others (e.g., Weaver and Gere, 1986).

Modeling Joints

Modification of Fixed-End-Forces

The truss considered in this study includes one of the following end conditions for members loaded with a uniformly distributed load (q):

- Both ends pinned
- Both ends rigid
- One end rigid and the other end semi-rigid

For the first two cases, derivations of the FEF are relatively straightforward and are given in text books (e.g., Weaver and Gere, 1986). The derivation of FEF for case c follows.

Figure 2a shows a prismatic beam element with a semi-rigid connection at one end (i-end) and rigid connection at the other (j-end). Let S_R be the rotational stiffness of the i-end. Rotational stiffness is defined as the moment per unit relative rotation (N-m/rad) at the connection. The length of the member is L, moment of inertia I, and E is the modulus of elasticity (MOE). The compatibility approach (Weaver and Gere, 1986) was used to derive FEF: R_1, R_2, M_1, and M_2 (see fig. 2a).

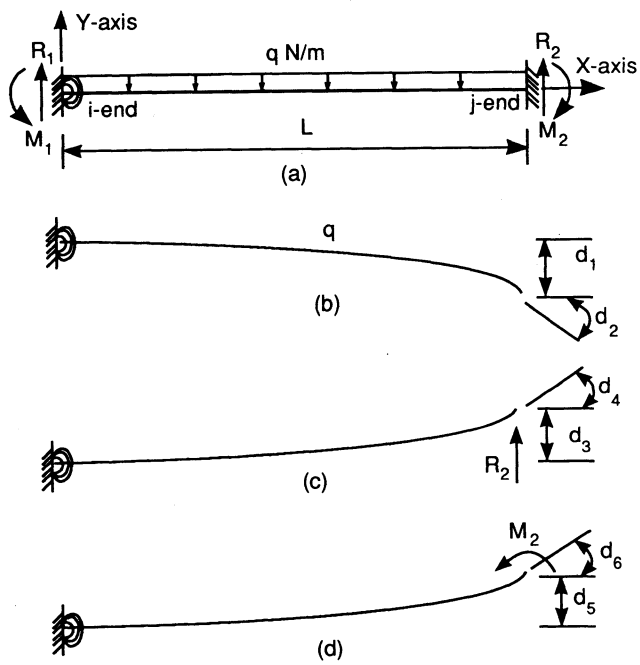

Figure 2–Beam with one end semi-rigid and the other end rigid: determination of the fixed-end-forces.

For the beam in figure 2a, the j-end is assumed free so that the reactions R_2 and M_2 are zero. This statically determinate beam is shown in figure 2b. Transverse deflection and rotation at the j-end are determined as follows.

Transverse deflection at the j-end, d_1, is composed of the following two parts:

1. Deflection due to load $q = -q L^4/8 E I$ (1)

2. Deflection due to the rotation at the i-end (semi-rigid effect)

   a. Moment at the i-end due to $q = -q L^2/2$ (2)

   b. Rotation at the i-end $= -q L^2/2 S_R$ (3)

   c. Transverse deflection at the j-end due to the rotation at the i-end $= (-q L^2/2 S_R)L$ (4)

Total transverse deflection at the j-end:

$$d_1 = (-q L^4/8 E I) - (q L^3/2 S_R) \quad (5)$$

Rotation at the j-end of the beam, d_2, is also composed of the following two parts:

1. Rotation due to the load q (no semi-rigid effect) $= -q L^3/6 E I$ (6)

2. Rotation at the j-end due to the rotation of the i-end caused by load q (same as in eq. 3) $= -q L^2/2 S_R$ (7)

Total rotation: $d_2 = -(q L^3/6 E I) - (q L^2/2 S_R)$ (8)

To prevent transverse deflection calculated in equation (5), apply a force R_2 at the j-end as shown in figure 2c. Transverse deflection and rotation at the j-end due to force R_2 are determined as follows.

Again, transverse deflection, d_3, consists of the following two parts:

1. Deflection due to $R_2 = R_2 L^3/3 E I$ (9)

2. Deflection due to rotation at the i-end caused by R_2

   Moment at the i-end $= R_2 L$ (10)

   Rotation at the i-end $= R_2 L/S_R$ (11)

   Deflection at the j-end $= R_2 (L/S_R) L$ (12)

Total transverse deflection due to R_2:

$$d_3 = (R_2 L^3/3 E I) + (R_2 L^2/S_R) \quad (13)$$

Rotation at the j-end, d_4, is also composed of the following two parts:

1. Rotation due to $R_2 = R_2 L^2/2 E I$ (14)
2. Rotation at the j-end due to the rotation of the i-end = $R_2 L/S_R$ (15)

Total rotation: $d_4 = (R_2 L^2/2 E I) + (R_2 L/S_R)$ (16)

To prevent rotation of equation 8, apply M_2 at the j-end as shown in figure 2d. Transverse deflection and rotation at the j-end due to M_2 are determined as follows.

Transverse deflection, d_5, is composed of the following two parts:

1. Deflection due to $M_2 = M_2 L^2/2 E I$ (17)
2. Deflection due to the rotation of the i-end:

   Moment at the i-end = M_2

   Rotation at the i-end = M_2/S_R

   Deflection at the j-end = $M_2 L/S_R$

Total deflection: $d_5 = (M_2 L^2/2 E I) + (M_2 L/S_R)$ (18)

Rotation at the j-end, d_6, is also composed of the following two parts:

1. Rotation due to $M_2 = M_2 L/E I$
2. Rotation due to the rotation of the i-end = M_2/S_R

Total rotation: $d_6 = (M_2 L/E I) + (M_2/S_R)$ (19)

Using compatibility relationships yields:

Eq. 5 = Eq. 13 + Eq. 18 (20)

and

Eq. 8 = Eq. 16 + Eq. 19 (21)

For convenience of writing equations:

Let $e_R = E I/L S_R$ and $e_1 = 1 + ie_R$; $i = 1, 2, 3, \ldots$.

Solving equation 20 and equation 21 for R_2 and M_2 yields:

$$R_2 = q L e_5/2 e_4 \quad M_2 = -q L^2 e_6/12 e_4 \quad (22)$$

Equations of static equilibrium can be used to find R_1 and M_1 by:

$$R_1 + M_1 = q L \quad (23)$$

Substituting R_2 for equation 22 into equation 23 and solving for R_1 yields:

$$R_1 = q L e_3/2 e_4$$

Summing moments about the j-end in figure 2a yields:

$$M_{j\text{-end}}: R_1 L - M_1 + M_2 - (q L^2/2) = 0 \quad (24)$$

Solving equation 24 for M_1 yields:

$$M_1 = q L^2/12 e_4$$

Therefore,

$$R_1 = q L e_3/2 e_4 \quad R_2 = q L e_5/2 e_4$$

$$M_1 = q L^2/12 e_4 \quad M_2 = -q L^2 e_6/12 e_4$$

The following limits are taken to check the previously derived relationships.

If i-end is rigid, then $S_R \to$ infinity as $e_R \to 0$ (Both ends rigid)

Take the limit of R_1, R_2, M_1, and M_2 as $e_R \to 0$

$R_1 = R_2 = q L/2$ and $M_1 = -M_2 = q L^2/12$ {ok}

If i-end is pinned, then $S_R \to 0$ as $e_R \to$ infinity (i-end pin and j-end rigid)

Take the limit of R_1, R_2, M_1, and M_2 as $e_R \to$ infinity

$R_1 = 3 q L/8$ $M_1 = 0$

$R_2 = 5 q L/8$ $M_2 = -q L^2/8$ {ok}

Modification of the Element Stiffness Matrix

The derivation of the ESM for a member with both ends semi-rigid follows. Figure 3a shows a prismatic beam-column element with semi-rigid connections at both ends. Let S_{Ri} (N-m/rad) and S_{Ai} (kN/m) be the rotational and axial stiffnesses of the i-end of the connection, respectively. Similarly, let S_{Rj} (N-m/rad) and S_{Aj} (kN/m) be the rotational and axial stiffnesses of the j-end of the connection, respectively. The length of the member is L, cross-sectional area is A, second moment of inertia about z-axis is I, and E is the MOE. The ESM has been derived in member coordinate system (x-y-z). Terms in the modified ESM were obtained using the flexibility approach (Weaver and Gere, 1986).

To obtain the flexibility coefficients at the j-end, the member is fixed at the i-end and free at the j-end as shown in figures 3b and 3c. A unit force is applied in the y-direction at the j-end as shown in figure 3b. Flexibility coefficients (D_{11} and D_{21}) of the j-end have been derived as follows.

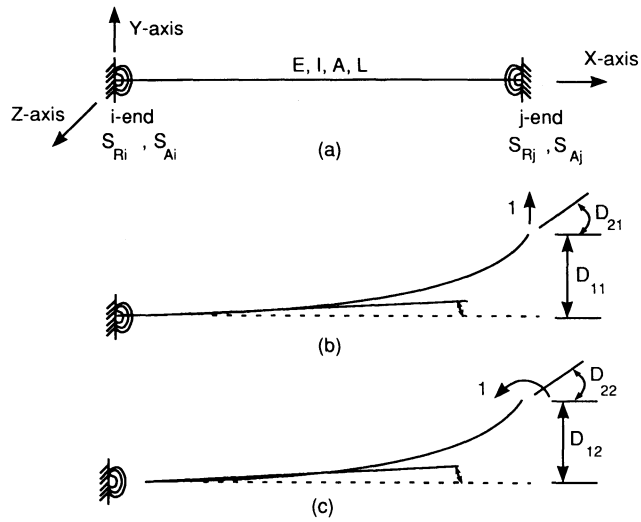

Figure 3–Beam with both ends semi-rigid: determination of the element-stiffness-matrix.

The transverse displacement at the j-end due to the unit force is denoted by D_{11} and is composed of the following two parts:

1. Displacement due to the unit force = $L^3/3EI$ (25)

2. Displacement due to the rotation at the i-end caused by the unit force:
   a. Moment at the i-end = $1 \times L$ (26)

   b. Rotation at the i-end = $1 \times L \times 1/S_{Ri}$ (27)

   c. Displacement at the j-end = $1 \times L \times 1/S_{Ri} \times L$ (28)

Therefore, $D_{11} = L^3/3EI + L^2/S_{Ri}$ (29)

The rotation of the j-end due to the unit force is denoted by D_{21} and is composed of the following two parts:

1. Rotation due to the unit force = $L^2/2EI$ (30)

2. Rotation due to the rotation of the i-end (as in eq. 27) = $1 \times L \times 1/S_{Ri}$

Therefore, $D_{21} = L^2/2EI + L/S_{Ri}$ (31)

Now apply a unit moment about the z-axis at the j-end as shown in figure 3c. Flexibility coefficients (D_{12} and D_{22}) of the j-end are derived as follows.

The transverse displacement at the j-end due to the unit moment at the i-end is denoted by D_{12} and is composed of the following two parts:

1. Displacement due to the unit moment = $L^2/2EI$ (32)

2. Displacement due to rotation of the i-end:

   a. Moment at the i-end = 1 (33)

   b. Rotation at the i-end = $1 \times 1/S_{Ri}$ (34)

   c. Displacement at the j-end = $1 \times 1/S_{Ri} \times L$ (35)

Therefore, $D_{12} = (L^2/2EI) + (L/S_{Ri})$ (36)

The rotation of the j-end due to a unit moment at the j-end is denoted by D_{22} and is composed of the following three parts:

1. Rotation due to the unit moment = L/EI (37)

2. Rotation due to the rotation at the i-end = $1/S_{Ri}$

3. Rotation due to the rotation of the j-end = $1/S_{Rj}$ (38)

Therefore, $D_{22} = (L/EI) + (1/S_{Ri}) + (1/S_{Rj})$ (39)

For convenience of writing equations and later matrices, the following non-dimensional parameters have been introduced:

$$e_{Ri} = EI/LS_{Ri}; \quad e_{Rj} = EI/LS_{Rj}; \quad e_{Rij} = 1 + e_{Ri} + e_{Rj}; \tag{40}$$

$$e_{Ri1} = 1 + e_{Ri}; \quad e_{Rj1} = 1 + e_{Rj}; \quad e_{Ri2} = 1 + 2\,e_{Ri}; \quad e_{Rj2} = 1 + 2e_{Rj}; \text{ etc...} \tag{41}$$

After substituting equations 40 and 41 into 29, 31, 36, and 39 and simplifying, the flexibility coefficients become:

$$D_{11} = L^3 e_{Ri3}/3EI; \quad D_{21} = L^2 e_{Ri2}/2EI;$$
$$D_{12} = L^2 e_{Ri2}/2EI; \quad D_{22} = L e_{Rij}/EI.$$

The flexibility matrix, $[F_j]$, for the j-end becomes

$$[F_j] = \begin{bmatrix} D_{11} & D_{12} \\ D_{21} & D_{22} \end{bmatrix} = \frac{L}{6EI} \begin{bmatrix} 2L^2 e_{Ri3} & 3L e_{Ri2} \\ 3L e_{Ri2} & 6 e_{Rij} \end{bmatrix} \tag{42}$$

Inversion of matrix $[F_j]$ in equation (42) yields the stiffness matrix, $[S_{jj}]$, for the j-end:

$$[S_{jj}]\, C \begin{bmatrix} 6e_{Rij} & -3Le_{Ri2} \\ -3Le_{Ri2} & 2L^2 e_{Ri3} \end{bmatrix} \tag{43}$$

$$\text{Where, } C = \frac{2EI}{L^3\left[\, 4e_{Rij} + 3\left(4e_{Ri}\, e_{Rj} - 1 \right)\right]}$$

The complete stiffness matrix, $[S'_M]$, without the axial stiffness (i.e., excluding column effect) is given by (Weaver and Gere, 1986):

$$[S'_M] = \begin{bmatrix} S_{ii} & S_{ij} \\ S_{ji} & S_{jj} \end{bmatrix} \quad (44)$$

where: $[S_{ii}]$, $[S_{ij}]$, $[S_{ji}]$, and $[S_{jj}]$ are all 2×2 submatrices of $[S'_M]$. The terms in $[S_{jj}]$ are defined as the restraint actions at the j-end of the member due to unit displacements at the same end. The terms in $[S_{ij}]$ are restraint actions at the i-end due to unit displacements at the j-end, and they are in equilibrium with the terms in $[S_{jj}]$. The terms in $[S_{ji}]$ consist of restraint actions at the j-end due to unit displacement at the i-end. The terms in $[S_{ii}]$ are restraint actions at the i-end due to unit displacements at the i-end, and they are in equilibrium with the terms in $[S_{ji}]$.

The matrix $[S_{jj}]$ has already been found and given by equation (43). The other three submatrices of $[S'_M]$ can be found by the transformation of axis. Statically equivalent forces at the i-end may be computed using the transformation matrix, [T], where [T] is:

$$[T] = \begin{bmatrix} 1 & 0 \\ L & 1 \end{bmatrix} \quad (45)$$

Then terms in submatrix $[S_{ij}]$ can be determined from the relationship: $[S_{ij}] = -[T][S_{jj}]$. This yields:

$$[S_{ij}] = C \begin{bmatrix} -6e_{Rij} & 3Le_{Ri2} \\ -3Le_{Rj2} & L^2 \end{bmatrix} \quad (46)$$

Because the ESM, $[S'_M]$, is symmetric, the submatrix $[S_{ji}]$ must be equal to the transpose of $[S_{ij}]$. Thus, solving $[S_{ji}] = [S_{ij}]^T$ yields:

$$[S_{ji}] = C \begin{bmatrix} -6e_{Rij} & -3Le_{Rj2} \\ 3Le_{Ri2} & L^2 \end{bmatrix} \quad (47)$$

The remaining submatrix $[S_{ii}]$ can be found from $[S_{ji}]$ using the relationship: $[S_{ii}] = -[T][S_{ji}]$. This yields:

$$[S_{ii}] = C \begin{bmatrix} 6e_{Rij} & 3Le_{Rj2} \\ 3Le_{Rj2} & 2L^2e_{Rj3} \end{bmatrix} \quad (48)$$

All the submatrices of $[S'_M]$ (eq. 44) have been determined. This completes the ESM of a member without including axial stiffness, which is the column effect. The ESM is given by:

$$[S'_M] = C \begin{bmatrix} 6e_{Rij} & 3Le_{Rj2} & -6e_{Rij} & 3Le_{Ri2} \\ 3Le_{Rj2} & 2L^2e_{Rj3} & -3Le_{Rj2} & L^2 \\ -6e_{Rij} & -3Le_{Rj2} & 6e_{Rij} & -3Le_{Ri2} \\ 3Le_{Ri2} & L^2 & -3Le_{Ri2} & 2L^2e_{Ri3} \end{bmatrix} \quad (49)$$

To include the column effect, consider an axial force member having elastic (semi-rigid) connections at both ends, as shown in figure 4a. Let the axial stiffness of the i-end and the j-end be denoted by S_{Ai} and S_{Aj}, respectively. Again, the flexibility method has been used to derive the ESM. Apply a unit force in the x-direction at the j-end (as shown in fig. 4b) and write the displacement at the same end. This displacement is made up of the following three components:

1. Displacement at the i-end due to the axial elastic connection at the i-end = $1/S_{Ai}$
2. Displacement at the i-end due to the axial elastic connection at the j-end = $1/S_{Aj}$
3. Elongation of the member = L/AE

Therefore, the total displacement,

$$d = L/AE + 1/S_{Ai} + 1/S_{Aj} \quad (50)$$

For convenience of writing equations and later matrices, the following non-dimensional parameters are introduced:

$$e_{Ai} = EA/LS_{Ai}; \qquad e_{Aj} = EA/LS_{Aj};$$
$$e_{Aij} = 1 + e_{Ai} + e_{Aj} \quad (51)$$

Substituting equation (51) into equation (50) yields

$$d = Le_{Aij}/AE \quad (52)$$

The term d in equation 52 is the flexibility matrix for the j-end. Inversion of d yields the ESM, $[K_j]$, for the j-end, as shown next.

$$[K_j] = [d]^{-1} = AE/Le_{Aij} \quad (53)$$

The transformation matrix, [T], is given by:

$$[T] = [1] \quad (54)$$

Now following the same procedure as used in deriving $[S'_M]$, the ESM for the axial force member having an elastic connection at both ends is given by:

$$[K'_M] = \frac{AE}{Le_{Aij}} \begin{bmatrix} 1 & -1 \\ -1 & 1 \end{bmatrix} \quad (55)$$

Combining $[S'_M]$ in equation 49 and $[K'_M]$ in equation 55 gives the following ESM for a beam-column element having an elastic connection at both ends:

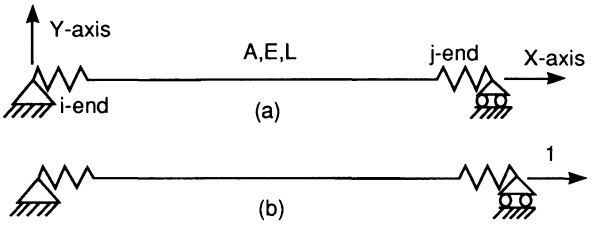

Figure 4–Beam with flexible axial connections: determination of the element-stiffness-matrix.

$$[S_M] = \begin{bmatrix} \frac{AE}{Le_{Aij}} & 0 & 0 & -\frac{AE}{Le_{Aij}} & 0 & 0 \\ 0 & 6Ce_{Rij} & 3CLe_{Rj2} & 0 & -6Ce_{Rij} & 3CLe_{Ri2} \\ 0 & 3CLe_{Rj2} & 2CL^2e_{Rj3} & 0 & -3CLe_{Rj2} & CL^2 \\ -\frac{AE}{Le_{Aij}} & 0 & 0 & \frac{AE}{Le_{Aij}} & 0 & 0 \\ 0 & -6Ce_{Rij} & -3CLe_{Rj2} & 0 & 6Ce_{Rij} & -3CLe_{Ri2} \\ 0 & 3CLe_{Ri2} & CL^2 & 0 & -3CLe_{Ri2} & 2CL^2e_{Ri3} \end{bmatrix} \quad (56)$$

Element stiffness matrices for other end conditions are determined from equation 56 by taking appropriate limits. For example, for both ends rigid, $S_{Ri} = S_{Rj} = \infty$ and $S_{Ai} = S_{Aj} = \infty$. Then C becomes $2EI/L^3$ and $e_{Ri} = e_{Rj} = 0$; $e_{Ai} = e_{Aj} = 0$; $e_{Rij} = e_{Ri1} = e_{Rj1} = 1$; and $e_{Aij} = 1$. Substituting the above conditions into equation 56 yields:

$$[S_M] = \begin{bmatrix} \frac{AE}{L} & 0 & 0 & -\frac{AE}{L} & 0 & 0 \\ 0 & \frac{12EI}{L^3} & \frac{6EI}{L^2} & 0 & -\frac{12EI}{L^3} & \frac{6EI}{L^2} \\ 0 & \frac{6EI}{L^2} & \frac{4EI}{L} & 0 & -\frac{6EI}{L^2} & \frac{2EI}{L} \\ -\frac{AE}{L} & 0 & 0 & \frac{AE}{L} & 0 & 0 \\ 0 & -\frac{12EI}{L^3} & -\frac{6EI}{L^2} & 0 & \frac{12EI}{L^3} & -\frac{6EI}{L^2} \\ 0 & \frac{6EI}{L^2} & \frac{2EI}{L} & 0 & -\frac{6EI}{L^2} & \frac{4EI}{L} \end{bmatrix} \quad (57)$$

Similarly, the ESM for other connections (e.g., one end rigid and the other semi-rigid) can be derived by taking appropriate limits.

Comparison of Joint Models

Truss

A fink truss, which is the most commonly used metal-plate-connected wood truss in light frame residential construction, was analyzed in this study (see fig. 1). The truss has a 5:12 slope, 8.53-m (28-ft) span (L), and is spaced 0.61 m (2 ft) on center. All truss members were 38 × 89 mm (2 × 4 in.) SP No. 2 KD 15 and were connected by 20-gage punched metal plates. Two 76 × 127-mm (3 × 5 in.) plates were used for each heel joint and web joint at the bottom chord and two 76 × 102-mm (3 × 4 in.) plates were used for the tension splice joints. The loads used to analyze the truss are summarized in figure 1. Load duration factor of 1.15 was used in this study.

Analysis Methods

The truss shown in figure 1 was analyzed for the following three different joint models:

Truss type analysis (PP). Web members are pinned at both ends to continuous top and bottom chords. The ridge, heel, and tension splice joints are all assumed as pinned.

Frame type analysis (RR): Web members are pinned to continuous top chords and the ridge joint is pinned. The heel, tension splice, and web at the bottom chord joints are assumed as rigid.

Semi-rigid analysis (SR): Web members are pinned to continuous top chords. The ridge joint is pinned. The heel, tension splice, and web at the bottom chord joints are assumed as semi-rigid (i.e., these joints have some axial and rotational stiffnesses).

For all three cases, top chords are continuous at nodes 2 and 6 and bottom chords are continuous at nodes 3 and 7, as shown in figure 1.

In farm trusses with large chord sizes, the effect of eccentricities may be significant and should be taken into account. In this study, the member sizes were small (2 × 4 in.) and effect of eccentricities may not be significant. Therefore, to simplify the analysis, we assumed that there were no eccentricities, i.e., the center lines of

TABLE 1. Joint stiffnesses

Joint	Axial Stiffness (lb/in.)	Rotational Stiffness (lb-in./rad)
Heel	15.0×10^5	38.0×10^5
Tension	3.0×10^5	2.4×10^5
Web	2.4×10^5	2.0×10^5

members met at a common point. We analyzed the truss for the design loads shown in figure 1. The allowable stress values [bending (repetitive) = 1750 psi (12.1 MPa); compression = 1150 psi (8.0 MPa); tension = 900 psi (6.2 MPa); shear = 95 psi (0.7 MPa)] of members were taken from the National Design Specification for Wood Construction (National Forest Products Association, 1986a). The joint stiffnesses, obtained experimentally from load-deflection and moment-rotation curves, were represented by their mean values (Gupta, 1990). The joint stiffness values are given in Table 1. The method used here is for the analysis of structures that are linear and elastic although it can be adopted to nonlinear analysis.

Results and Discussion

The maximum deflection (downward Y-deflection) of the truss was compared for the three joint models. Displacements at the web joints, tension splice joints, and heel joints in the bottom chord for all three joint models are shown in Table 2. The predicted response of the truss varies greatly depending on the joint model. In a comparison of maximum deflection between RR and SR, the SR joint model predicted 24% higher deflection. Rotation of the heel joint was also 7% higher for SR. This result was to be expected because the truss with the stiffer connections (RR) would displace less under the same load than the truss with more flexible connections (SR).

The maximum deflection for PP was 15.78 mm (L/541), whereas for SR it was 10.39 mm (L/822), a decrease of 34%. The value for maximum deflection for SR was between values for the RR and PP, but closer to that for RR, indicating that the semi-rigid joint model, which is more realistic, is closer to the rigid joint model based on the maximum deflection of the truss. Member forces and combined stress interaction (CSI) indices for the critical (most highly stressed) member near the heel joint of the top and bottom chords for RR were compared with those for SR.

TABLE 2. Comparison of predicted joint displacements from each of the three models

Displacement	Method of Analysis PP	RR	SR
Web at the bottom chord joint (Y-displacement, mm)	6.64 (0.2614)*	6.42 (0.2528)	6.94 (0.2732)
Tension splice joint (maximum Y-displacement of truss, mm)	15.78 (0.6213)	8.35 (0.3287)	10.39 (0.4091)
Heel joint (rotation, rad)	0.01307	0.01115	0.01195

* Displacement in inches.

The CSI was calculated at a point where combination of moment and axial force produced maximum CSI along the length of a member. The effective column length was determined as outlined in the National Forest Products Association (NFPA, 1986b). All the members with semi-rigid ends were assumed rigid for the purpose of determining effective column length because no procedure exists for calculating effective column length for a member with semi-rigid ends. Also, as shown earlier based on the maximum deflection of the truss, semi-rigid joint assumption is closer to rigid joint assumption.

A comparison of the internal forces in the top and bottom chords indicates that axial forces and moments for SR and RR joint models are different (as shown in Table 3). The difference between axial forces was small, but the difference between moments was practically significant. For example, the moment (also the maximum moment in the truss) at the i-end of member 6-8 changed from 567 N-m for the rigid assumption to 493 N-m for the semi-rigid assumption, a reduction of 13%. This shows that the rotational stiffness due to slip at the joint influenced the bending moment of the joint. Shear forces were very small and their values either increased or decreased by an insignificant amount because shear stiffness of the joints was not considered.

As expected for a triangular truss, the maximum combined stress indices for the top and bottom chords occurred at the exterior panels. The top and bottom chords were assumed to be braced laterally. For member 6-8, the CSI index was 1.28 for SR, 1.42 for RR, and 1.45 for PP (as shown in Table 3). Reduced CSI index for member 6-8 was mainly due to the reduced bending moment in the member. The SR model resulted in a reduced CSI index for the top chord, but for the bottom chord the index remained very similar to those for the other two models. The same adjusted allowable stresses were used to calculate the CSI indices for all assumptions.

The predicted truss behavior, based on maximum deflection, is primarily affected by the joint model used in the analysis. By incorporating semi-rigidity into the analysis and design of trusses, an engineer could assess the influence of different connection models on the predicted performance of trusses.

TABLE 3. Forces at i- and j-ends and CSI in a top chord member (6-8) and bottom chord member (1-3)

Force	End	Member 6-8 SR	RR	PP	Member 1-3 SR	RR	PP
Axial (N)*	i-end	11583	11677	11726	-11178	-11276	-11339
	j-end	-12482	-12575	-12629	11178	11277	11339
Shear (N)	i-end	1259	1299	1335	294	297	311
	j-end	903	867	827	538	535	520
Moment (N-m)†	i-end	493	567	584	-82	-69	0
	j-end	-82	-69	0	-270	-268	296
CSI‡		1.28	1.42	1.45	0.84	0.85	0.89

* 1 N = 0.225 lbf.
† 1 N-m = 8.851 lbf-in.
‡ For adequate design, the CSI values should be less than or equal to 1.0 (National Forest Products Association, 1986).
The analysis in this study is only meant for comparison.

SUMMARY

Metal-plate-connected wood trusses are common in residential, commercial and agricultural buildings. Improvements in the analysis and design of trusses to make them more cost effective would, therefore, have a significant impact on the truss industry. One way to produce more cost effective trusses is to use advanced analysis and design methods for these trusses. Advanced methods of analyzing trusses include using more realistic representations of joint behavior and variation in material properties. A more realistic representation of semi-rigid joint behavior in a matrix method of truss analysis was considered. Instead of using fictitious members to represent joints, the element-stiffness matrix and fixed-end forces were modified to include semi-rigidity of joints. In terms of usage, this is a simplified approach because it does not require estimation of the dimensions of the fictitious members according to joint stiffnesses. It is a more accurate approach because it is based on direct stiffness method to include the semi-rigid behavior of joints. The method presented here is based on direct stiffness method which is a powerful analysis tool for framed structures of any type with a high degree of accuracy. Including the stiffness of the joints in analyzing trusses will predict the behavior of trusses more accurately. As shown here, the predicted response of the truss depends on the joint assumption. The predicted maximum deflection of the truss with the semi-rigid joint assumption was 34% less than that for the same truss with a pinned-joint assumption. The predicted maximum moment in the truss with semi-rigid joint assumption was 13% less than that for the same truss with rigid-joint assumption. This approach can be used to analyze other structures when the strength and stiffness values of joints are known. The external load can be treated as a determinate quantity or as a random variable.

REFERENCES

Cramer, S. M. and R. W. Wolfe. 1989. Load-distribution model for light-frame wood roof assemblies. *J. Structural Eng.* 115(10):2603-2616.

Foschi, R. O. 1977. Analysis of wood diaphram and trusses. Part II: Truss plate connection. *Can. J. Civil Eng.* 4(3):353-362.

Fu, H. C. and M. Seckin. 1988. Rigidity evaluation of wooden warren truss connections. In *Proc. of the 1988 International Conference on Timber Engineering*, ed. R. Y. Ltani, Vol. 2, 121-130. Forest Products Res. Soc.

Gupta, R. 1990. Reliability analysis of semi-rigidly connected metal plate residential wood trusses. Ph.D. thesis (unpublished), Cornell University, Ithaca, NY.

Lau, P. W. C. 1987. Factors affecting the behavior and modeling of toothed metal-plate joints. *Can. J. Civil Eng.* 14(2):183-195.

Maraghechi, K. and R. Y. Itani. 1984. Influence of truss plate connectors on the analysis of light frame structures. *Wood Fiber Sci.* 16(3):306-322.

Masse, D. I. and J. J. Salinas. 1988. Analysis of timber trusses using semi-rigid joints. *Can. Agric. Eng.* 30(1):111-124.

National Forest Products Association. 1986a. Design values for wood construction (supplement). Washington, DC: NFPA.

National Forest Products Association. 1986b. National design specification for wood construction. Washington, DC: NFPA.

Sasaki, Y., S. Miura and T. Takemura. 1988. Non-linear analysis of semi-rigid jointed metal-plate wood truss. *J. of the Japanese Wood Research Society* 34(2):120-125.

Triche, M. H. and S. K. Suddarth. 1988. Advanced design of metal plate connector joints. *Forest Products Journal* 38(9):7-12.

Truss Plate Institute. 1985. Design specification for metal plate connected wood trusses-TP1-85. Madison, Wl.

Weaver W. W., Jr. and J. M. Gere. 1986. *Matrix Analysis of Framed Structures*. New York: Van Nostrand Reinhold Company, Inc.